POSEIDON-BERICHTE

Benthic-pelagic coupling in sandy sediment regions and its interactions with the biological carbon in the open ocean

Cruise No. POS531

18.01.2019 – 01.02.2019
Las Palmas (Canary Islands) – Mindelo (Kap Verden)

Benthic-pelagic coupling in sandy sediments

Iversen, M. H., Swoboda, S., Marchant, H., Ahmerkamp, S., Schwalfenberg, K., Hehemann, J., Buck-Wiese, H., Stock, L., Bolte, A., Bäger, J.

Chief Scientist: Morten Hvitfeldt Iversen

MARUM and University of Bremen, Leobener Strasse 13, Bremen

Alfred Wegener Institute for Polar and Marine Research, Am Handelshafen 12, Bremenhaven

2019

Table of Contents

1 Cruise Summary 1

2 Participants 6

3 Preliminary Results 7

3.1 Oceanography 7

3.1.1 Rosette with CTD-oxygen-fluorescence probe and the Secchi disk…….....7
(Kai Schwalfenberg, Soeren Ahmerkamp, Steffen Swoboda, Hannah Marchant, Jan-Hendrik Hehemann, Jana Bäger, Alek Bolte, Hagen Buck-Wiese, Lennart Stock, and Morten Iversen)

3.1.2 Dissolved Nutrients……..…….....9
(Hannah Marchant and Jana Bäger)

3.2 Marine Glycobiology – Drivers of dissolved and particulate glycan concentrations 12
(Hagen Buck-Wiese, Alek Bolte, Lennart Stock, and Jan-Hendrik Hehemann)

3.3 Particle Flux Studies – Upper ocean particle flux measured with free-drifting sediment traps 16
(Steffen Swoboda, Arjun Chennu, and Morten Iversen)

3.4 Optical Particle Studies – Vertical profiles of marine snow aggregates with the In Situ Camera (ISC) 21
(Steffen Swoboda and Morten Iversen)

3.5 Marine Microbiology – Size-specific sinking velocities and microbial respiraiton 23
(Steffen Swoboda and Morten Iversen)

3.6 Benthic Primary Production, Carbon Remineralization, and Nitrogen Cycling..... 25
(Soeren Ahmerkamp, Hannah Marchant, and Kai Schwalfenberg)

4 Station List 29

5 Acknowledgements 33

6 References 33

1 Cruise summary

(Morten Iversen)

The research cruise POS 531 is the first research cruise within the MARUM Excellence Cluster 'The Ocean Floor – Earth's Uncharted Interface'. The scientific party consisted of scientists from MARUM, Max Planck Institute for Marine Microbiology, University of Bremen, Institute of Chemistry and Biology of the Marine Environment, Carl von Ossietsky Universität Oldenburg, and Alfred Wegener Institute for Polar and Marine Research.

The research aim of POS 531 was to investigate carbon and nitrogen cycling in sandy shelf sediments off the coast of Morocco in order to better understand their influence on pelagic primary production and lateral transport to the open ocean. This will allow us to better understand the role of primary production in sandy shelf regions for open ocean carbon sequestration.

The transfer of organic matter from the surface ocean to the ocean floor is a key regulator of atmospheric carbon dioxide (CO_2) as well as the exclusive food source for life in vast areas in the deep sea, and the main pathway for the long-term storage of carbon in the sediments. However, the mechanisms of transformation, degradation, and preservation of organic matter within the water column and at the seafloor are hardly understood. Algal blooms form dissolved and particulate organic matter, which together with (bio)minerals aggregate into settling particles that shuttle carbon and other elements to the deep ocean. Along its vertical path, this flux is rapidly attenuated by microbial activity, making the oceans a "gigantic heterotrophic digester" that is directly tied to atmospheric carbon dioxide levels. Our understanding of chemical transformation processes and the origin and age of settling particles is insufficient due to the inherent chemical complexity of organic matter in the ocean and the poorly constrained transport mechanisms of organic matter and (bio)minerals through the water column and at the sea floor. The magnitude of export depends on how the particle flux is transformed as it falls. To understand the functioning of the ocean's biology and chemistry, we need to understand what controls both the horizontal and vertical transport of material through the water column.

RV Poseidon left the port of Las Palmas, Gran Canaria, Spain, on 18th January 2019 at 09:00 on schedule and started the voyage in a SW direction towards our study area off the coast of Morocco. Sunday morning on the 20th January we started our station work at the off-shore long-term mooring site 'CB' at 17:00. We deployed one CTD Rosette and two In Situ Camera profiles to identify the different water masses and record the vertical distribution of settling aggregates through the water column. We further recorded water currents and backscattering with an ADCP (Acoustic Doppler Current Profiler), which was provided and equipped on RV Poseidon by colleagues from GEOMAR.

Monday morning (21.01.2019) at 09:00, we continued our work at station CB and deployed our first drifting array DF-20. The drifting array consisted of four cylindrical sediment traps at each of three depths; 100, 200 and 400 m. One of the four cylinders at each depth was filled with a viscous gel to preserve the shape and structure of the fragile settling particles. Thereafter we investigated the particle dynamics through the water column by deployments of three CTD Rosettes, one Secchi-disk, three In Situ Camera profiles, several hand nets for zooplankton sampling, and one Marine Snow Catcher. Station work ended at 23:00.

The Marine Snow Catcher collects small in situ formed organic aggregates. We measured the small scale activities within those aggregates on board and could directly measure the rate at which bacteria and other microorganisms degraded the organic matter and respired it back to CO_2. In parallel we determined the settling velocity of each of the collected aggregates and could thereby determine how fast the aggregate sank in relation to how fast the microorganisms respired organic matter. If respiration occurs in the surface ocean, the CO_2 will immediately be exchanged with the atmosphere, however, if the majority of this respiration occurs at depths below 1000 m then the CO_2 will be stored in the ocean for hundreds of years.

From Monday morning at 09:00 (21.01.2019) to Tuesday at 09:00 we conducted the first 24 hour diel cycle experiment measuring algal production and zooplankton at the CB station to compare the light driven production rhythm of microalgae with the feeding rhythm of zooplankton. We took samples every hour through the ship inlet pump from the upper 10 m of the water column. In addition we obtained water from the CTD at 10 AM, 4 PM, 4 AM from five different depths. The water samples were filtered to obtain particulate organic matter for carbon and nitrogen analysis. The filtered seawater was extracted with affinity chromatography to measure dissolved energy molecules such as carbohydrates that are an important food source for bacterio-plankton. In addition to these water samples we deployed a zooplankton net every hour to collect crustaceans and other organisms feeding on microalgae. In parallel we conducted on deck incubation experiments where we incubated microalgae with ^{13}C-DIC to obtain assimilation rates during the light and dissimilation rates during the dark phase.

Tuesday (22.01.2019) at 04:00 we continued the station work with two deployments of the CTD Rosette, two In Situ Camera profiles, one Secchi-disk, and the recovery of the drifting array (DF-20).

Wednesday (23.01.2019) at 16:00 we arrived at the shallow shelf station where we investigated the sediment and water column processes. This was done by deployments of several Van Veen Grabs, one In Situ Camera, one CTD Rosette, one Marine Snow Catcher, several Sediment Multi-Corers, several zooplankton hand nets, and the 24 hours deployment of the LanceALot benthic lander. The lander was equipped with scanners that recorded the seafloor typography, pigment composition, and oxygen distribution. The station work ended at 21:00.

Sediment collected with the Van der Veen Grab was packed into flow through reactors and subsequently oxygen consumption rates were measured and incubations were carried out using stable isotope tracers to determine nitrogen cycling rates. This data will be combined with in-situ data collected using the benthic lander to determine areal fluxes of oxygen consumption and nitrogen loss. The MUC cores were used to determine the release of FDOM from the sediment and the flow velocity needed to resuspend the sediment and microphytobenthos. When combined this provides valuable information on the fate of material reaching the sandy seafloor.

Thursday (24.01.2019) we started with Van Veen Grabs at 06:30 to sample the sediment in the dark in order to prepare for incubations for benthic primary production. Hereafter we deployed two CTD Rosettes, one In Situ Camera, a Secchi-disk, and a Marine Snow Catcher before we recovered the LanceALot. At 15:00 we ended the work at the shallow station and steamed towards our slope station.

Friday (25.01.2019) we started the work at the slope station at 09:00 where we deployed the next drifting array (DF-21). Hereafter we deployed three CTD Rosettes, three In Situ Cameras, one Secchi-disk, several zooplankton hand nets, and one Marine Snow Catcher. The station work ended at 23:00.

From Friday morning at 09:00 (25.01.2019) to Saturday at 9:00 we conducted the second 24 hour diel cycle experiment measuring algal production and zooplankton at the 600 m slope station. We took samples every hour through the ship inlet pump. In addition we obtained water from the CTD at 10 AM, 4 PM, 4 AM from five different depths. The water samples were filtered to obtain particulate organic matter for carbon and nitrogen analysis. The filtered seawater was extracted with affinity chromatography. In addition to these water samples we deployed the zooplankton net every hour. In parallel we conducted on deck incubation experiments where we incubated microalgae with 13C.

Saturday (26.01.2019) we started our station work at 04:00 with one CTD Rosettes, thereafter, we deployed two In Situ Camera profiles and recovered the drifting array. The station work at the slope station ended at 10:30. Thereafter we started our transect work from the slope station to the 30 m shelf station. This was in total 6 transect stations with a CTD Rosette and an In Situ Camera deployed at each of them. The lmADCP was also running during both the long-term stations and the transect. We ended the transect work at 22:00.

Sunday (27.01.2019) at 08:00 we started the work at the 60 m shelf station. We first deployed two CTD Rosettes and 10 Van Veen Grabs, to both collect water for incubations and to survey the sediment to test if it was sandy before we deployed the LanceALot lander. At 10:30 we deployed the LanceALot and thereafter we stayed near the lander to study the biogeochemical processes in both the water column and the sediment. This was done by deploying four In Situ Cameras, one Secchi-disk, one Marine Snow Catcher, four Sediment Multi-Corers, and several zooplankton hand nets. The station work ended at 23:00.

At the 60 m shelf station the incubations for benthic processes were repeated. The sandy seafloor at this station was less permeable compared the previous shelf station, and initial experiments suggested that oxygen consumption rates were substantially higher.

Simultaneously, from Sunday (27.01.2019) morning at 09:00 to Monday at 9:00 we conducted the third 24 hour diel cycle experiment measuring algal production and zooplankton abundance. We took samples every hour through the ship inlet pump at a depth of about 5 m. In addition we obtained water from the CTD at 10AM, 4PM, 4AM from five different depth. The water samples were filtered to obtain particulate organic matter for carbon and nitrogen analysis. The filtered seawater was extracted with affinity chromatography to measure dissolved energy molecules. In addition to these water samples we deployed a zooplankton net at 10 AM, 4 PM, 9 PM and 10 PM to collect crustaceans and other organisms feeding on microalgae. In parallel we conducted on deck incubation experiments where we incubated microalgae with 13C.

Monday (28.01.2019) at 04:00 we continued the work at the 60 m shelf station and deployed two CTD Rosettes, one In Situ Camera, and one Van Veen Grab before we recovered the LanceALot at 10:30. Hereafter we started our transect stations towards the off-shore long-term monitoring station CBi.

Tuesday (29.01.2019) at 08:00 we deployed the last drifting trap (DF-22) at the CBi station. Additionally we deployed three CTD-Rosette profiles, four deployments of the In Situ Camera, one Secchi-disk, one Marine Snow Catcher, and several deployments of the zooplankton hand-net before we ended the station work at 22:00.

Wednesday (30.01.2019) we started the station work at 04:00 with a CTD-Rosette deployments and a deployment of the In Situ Camera before we recovered the drifting trap (DF-22) at 08:00. This ended the scientific work during the Poseidon cruise POS531 and at 09:00 we began our journey towards Mindelo, Cape Verde.

During the rest of Wednesday and Thursday we finished the last analyses in the laboratories and started packing and preparing for demobilization of the ship in Las Palmas. The pilot boarded Poseidon at 09:00 Monday the 1st of February. The container was packed and Poseidon was unloaded and cleaned before we returned back in Bremen Thursday the 4th of February in the evening.

During the cruise, we launched 161 instrument deployments: In Situ Camera (33x), Rosette-CTD (28x), Hand-net (58x), Marine Snow Catcher (6x), Bottom Water Samplers (3x), Van der Veen Grap (19x), LanceALot Lander (2x), Multi-Corer (4x), Secchi disc (5x), and Drifting Traps (3x). We had mostly calm weather and a relatively low swell of 1-3 m throughout the cruise. In summary, we had a successful cruise and our thanks and gratitude goes to Capt. Matthias Günther and his crew for supporting us.

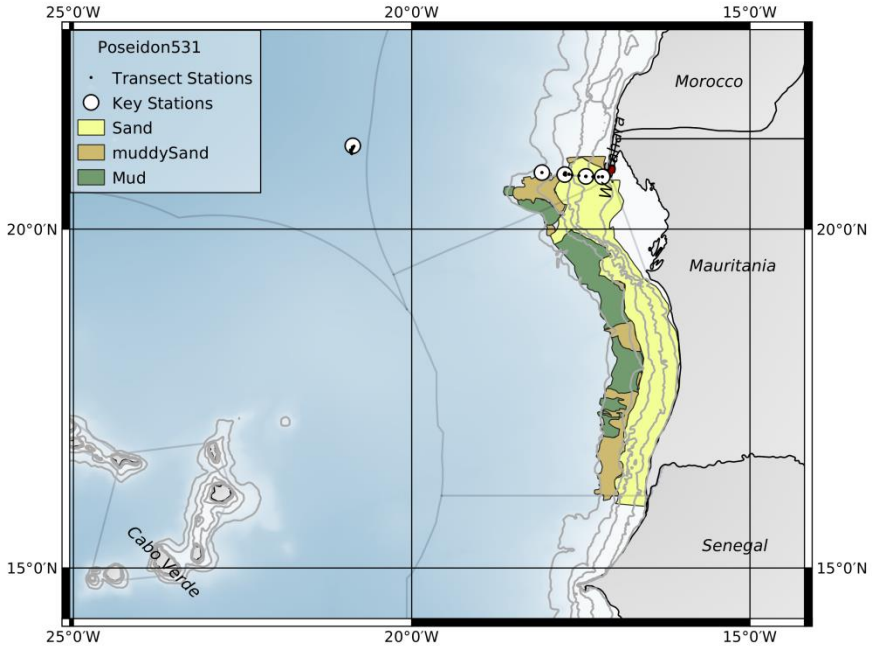

Fig. 2.1 Map of the key and transect stations during POS531.

2 Participants

Name	Discipline	Institution
Iversen, Morten H., Dr.	Chief Scientist	AWI/MARUM
Swoboda, Steffen	Scientist	MARUM
Marchant, Hannah, Dr.	Scientist	MPI
Ahmerkamp, Sören, Dr.	Scientist	MPI
Schwalfenberg, Kai	Scientist	ICBM
Hehemann, Jan-Hendrik, Dr.	Scientist	MARUM/MPI
Buck-Wiese, Hagen	Scientist	MARUM/MPI
Stock, Lennart	Technician	MARUM/MPI
Bolte, Alek	Technician	AWI
Bäger, Jana	Technician	AWI

MARUM	Center for Marine Environmental Sciences, University of Bremen, Germany
AWI	Alfred Wegener Institute for Polar and Marine Research, Bremerhaven, Germany
MPI	Max Planck Institute for Marine Microbiology, Bremen, Germany
ICBM	Institute for Chemistry and Biology of the Marine Environment, University of Oldenburg, Oldenburg

3 Preliminary Results

3.1 Oceanography

3.1.1 Rosette with CTD-oxygen-fluorescence probe and the Secchi disk

(Kai Schwalfenberg, Soeren Ahmerkamp, Steffen Swoboda, Hannah Marchant, Jan-Hendrik Hehemann, Jana Bäger, Alek Bolte, Hagen Buck-Wiese, Lennart Stock, and Morten Iversen)

Background

We recorded 28 vertical profiles with the shipboard Seabird CTD (see Table 3.1). Apart from the temperature, salinity and pressure sensors, the Seabird CTD was equipped with additional oxygen and fluorescence sensors and mounted on a rosette with 12 Niskin bottles, which each collected 8 L of water. Water samples were collected on all CTD-Rosette casts. The water samples were used for nutrient determinations, chl. a pigments, and to study diel shifts in polysaccharides (see section on Marine Glycobiology).

Table 0.1: List of Rosette-CTD (ROS + CTD) profiles and depths of water taken with the Niskin bottles of the rosette (ROS). Water samples were taken for determinations of nutrient concentrations, chl. a pigments, and polyssacharides.

Station No. GeoB	Latitude [N]	Longitude [W]	Water depth [m]	Water depths of samples [m]
23601_01	21°12.58	20°52.51	4154.4	4x14, 2x24, 2x43, 2x63, 2x100 – CTD 1<100 m
23601_07	21°12.58	20°52.13	4152.1	1x44, 1x103, 1x270, 1x 397, 1x666, 1x893, 2x1302, 2x2383, 2x2678, CTD <2700 m
23601_18	21°11.46	20°52.35	4150.4	1x18, 1x34, 1x53, 1x102, 1x199, 1x398 – CTD <400 m
23601_26	21°09.77	20°53.90	4190.1	1x44 1x101, 1x162, 1x330, 1x448, 1x538, 1x794 – CTD <800 m
23601_35	21°09.20	20°53.76	4150.6	1x15, 1x30, 1x65, 1x100, 1x200, 1x400, 1x1000, CTD <1000 m
23602_07	20°46.32	17°10.92	28	1x45, 1x99, 1x163, 1x202, 1x253, 1x418, 1x597, 1x794, 1x2074 – CTD <2100 m
23602_17	20°46.32	17°10.90	29.1	6x1700, 6x1800 – CTD <1850 m
23602_21	20°46.36	17°10.93	28.8	1x34, 1x63, 1x270, 1x418, 1x518, 1x793, 1x1715, 1x1816 – CTD <1800 m
23603_03	20°48.30	17°44.33	711.2	8x100, 2x200, 2x400 – CTD <400 m
23603_12	20°48.62	17°44.72	771.2	3x913, 3x1067, 3x1138, 3x1168 – CTD <1168 m
23603_21	20°47.84	17°43.62	632.1	1x30, 1x120, 2x240, 2x360, 2x460, 2x490, 2x548 – CTD<550 m
23603_28	20°49.16	17°44.50	747.6	Cable short-circuited
23604_02	20°48.59	17°40.59	423.1	2x51, 2x100, 2x179, 2x208, 2x245, 2x279 – CTD<290 m

23605_01	20°47.87	17°37.70	94.1	1x15, 2x30, 1x65, 2x100, 3x200, 2x325, 1x400 – CTD<400 m
23606_02	20°47.41	17°31.74	75.8	6x1700, 6x1800 – CTD <1850 m
23607_01	20°46.32	17°19.35	46.5	1x34, 1x63, 1x270, 1x418, 1x518, 1x793, 1x1715, 1x1816 – CTD <1800 m
23608_02	20°46.25	17°14.41	38.6	8x100, 2x200, 2x400 – CTD <400 m
23609_01	20°46.35	17°11.02	28.2	3x913, 3x1067, 3x1138, 3x1168 – CTD <1168 m
23610_01	20°46.62	17°25.70	58.7	1x30, 1x120, 2x240, 2x360, 2x460, 2x490, 2x548 – CTD<550 m
23610_12	20°46.72	17°25.66	59.2	Cable short-circuited
23610_21	20°46.75	17°25.54	59	2x51, 2x100, 2x179, 2x208, 2x245, 2x279 – CTD<290 m
23610_26	20°46.56	17°25.48	57.5	1x15, 2x30, 1x65, 2x100, 3x200, 2x325, 1x400 – CTD<400 m
23610_29	20°46.71	17°25.36	57.7	6x1700, 6x1800 – CTD <1850 m
23611_01	20°50.07	18°04.51	1567.7	1x34, 1x63, 1x270, 1x418, 1x518, 1x793, 1x1715, 1x1816 – CTD <1800 m
23612_02	20°50.84	18°24.29	2098.4	8x100, 2x200, 2x400 – CTD <400 m
23613_02	20°51.02	18°44.23	2610.7	3x913, 3x1067, 3x1138, 3x1168 – CTD <1168 m
23613_07	20°50.73	18°45.19	2724.2	1x30, 1x120, 2x240, 2x360, 2x460, 2x490, 2x548 – CTD<550 m
23613_10	20°51.26	18°48.82	2858	Cable short-circuited

Preliminary Results

The vertical CTD profiles were obtained along a transect in an off-shore. The different water layers were characterized by their temperature and salinity (Fig. 3.1). We additionally measured the Secchi depths at each key station.

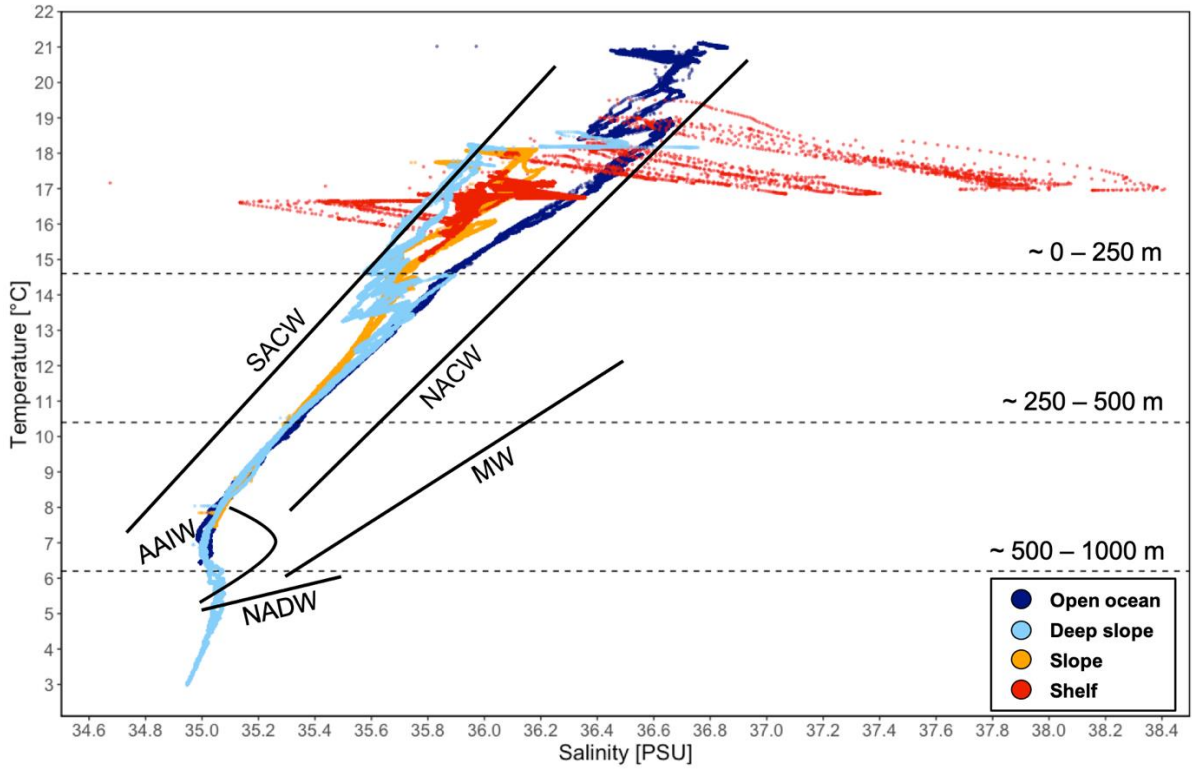

Fig. 3.1: Temperature and salinity plot to identify the different water masses that we sampled during POS531.

3.1.2 Dissolved Nutrients

(Hannah Marchant and Jana Bäger)

Background

Samples were taken for analysis of nitrate, nitrite, phosphate and silicate concentrations at the 4 main stations and all of the transect stations (Table 3.2). These samples were filled into 50 ml screw cap vials and returned to Bremen for analysis. Separate samples for ammonium analysis were collected in 50 ml screw-cap vials (Sarstedt, Germany). Ammonium was measured on-board and nutrient samples were frozen at -20 C for analysis in Bremen, Germany. The screw-top vials for ammonium were pre-cleaned with 10% HCl solution and washed once with seawater before collection of 40 mL seawater. For the 4 main stations 10 mL of OPA solution was added immediately to 40 ml of sample and measured after a reaction time of 3 hours. For the transect stations, samples were stored in the fridge for less than 12 hours and stations 23604-23608 were measured together, as were stations 23611 and 23612. For the last station (23613) the cartridge on the milliQ machine was full and therefore water with less than 2 nmol L^{-1} NH4 from station 23612 was used to prepare the standard series.

Table 3.2: GeoB- stations, event number, bottle number and sampling depth of CTD casts where nutrient samples were taken. Ammonium concentrations were subsequently determined on Board. When ammonium concentration was below detection limit it is indicated by 'b.d.l.'.

Station Name (GeoB-)	Bottle number (#)	Depth (m)	Ammonium concentration (nmol L-1)
23602-7	6	25	523.5
23602-7	7	21	499.3
23602-7	8	17	473.8
23602-7	9	13	321.2
23602-7	10	9	245.2
23602-7	11	5	248.0
23603-3	1	700	b.d.l.
23603-3	3	300	b.d.l.
23603-3	5	200	b.d.l.
23603-3	6	100	b.d.l.
23603-3	7	50	35.2
23603-3	9	24	48.3
23603-3	11	surface	104.8
23604-2	1	400	37.0
23604-2	3	300	12.0
23604-2	4	200	26.6
23604-2	6	100	36.5
23604-2	8	50	150.1
23604-2	10	25	104.1
23604-2	12	surface	137.2
23605-1	1	90	45.7
23605-1	3	75	19.0
23605-1	5	50	0.0
23605-1	7	25	24.4
23605-1	9	20	50.3
23605-1	11	surface	41.1
23606-2	1	68	226.6
23606-2	3	57	249.0
23606-2	5	50	178.8
23606-2	7	30	57.5
23606-2	9	13	49.8
23606-2	11	surface	34.0
23607-1	1	45	b.d.l.
23607-1	3	36	13.5
23607-1	5	25	46.8
23607-1	7	20	31.7
23607-1	9	11	18.2
23607-1	11	surface	96.2

23608-2	1	35	151.3
23608-2	3	25	14.6
23608-2	5	15,5	93.8
23608-2	7	12	1.7
23608-2	9	5	18.1
23608-2	11	surface	21.4
23609-1	1	27	128.7
23609-1	3	23	136.5
23609-1	5	18	105.8
23609-1	7	12	140.2
23609-1	9	7	91.9
23609-1	11	surface	85.8
23610-12	1		82.8
23610-12	3		11.6
23610-12	5		b.d.l.
23610-12	7		57.5
23610-12	9		17.4
23610-12	11		4.2
23611-1	1	1560	116.3
23611-1	2	1448	44.3
23611-1	3	1340	15.8
23611-1	4	1240	10.8
23611-1	5	700	37.1
23611-1	6	400	b.d.l.
23611-1	8	240	46.1
23611-1	9	120	67.7
23611-1	10	45	396.1
23611-1	11	31	651.8
23611-1	12	surface	355.5
23612-2	1	2090	37.6
23612-2	2	1780	b.d.l.
23612-2	3	1380	b.d.l.
23612-2	4	1000	b.d.l.
23612-2	5	799,5	b.d.l.
23612-2	6	600	26.5
23612-2	7	480	b.d.l.
23612-2	8	330	11.2
23612-2	9	199	b.d.l.
23612-2	10	41	265.9
23612-2	11	25	674.1
23613-2	2	2682	b.d.l.
23613-2	3	1950	127.2
23613-2	4	1450	b.d.l.
23613-2	5	1260	b.d.l.
23613-2	6	850	16.9

23613-2	7	450	b.d.l.
23613-2	8	255,5	b.d.l.
23613-2	9	119	b.d.l.
23613-2	10	79	b.d.l.
23613-2	11	25	524.2
23613-2	12	surface	474.2

3.2 Marine Glycobiology - Drivers of dissolved and particulate glycan concentrations

(Hagen Buck-Wiese, Alek Bolte, Lennart Stock, and Jan-Hendrik Hehemann)

Background

Photosynthesis in the surface ocean contributes almost half to global primary production. The Marine Gylcobiology group uses the glycan laminarin as our model system. Laminarin is a primary photosynthate of phytoplankton and is used intracellularly as central energy compound by diatoms, and also as a preferential substrate of heterotrophic bacteria (e.g. Teeling et al. 2012, Unfried et al. 2019). Intracellular laminarin leaks from diatom cells to the environment by excretion or passive diffusion (Carlson and Hansell 2015, Chen and Thornton 2015), through zooplankton grazing (Carlson and Hansell 2015), and viral lysis (e.g. Suttle et al. 2007, Breitbart et al. 2012). We recently published a method to unambiguously determine the concentration of laminarin via enzymatic digestion (Becker et al. 2017). Using this method, we found laminarin concentrations to increase to up to 25% of particulate organic carbon (POC) during the day and to decrease at night (Becker et al. submitted). However, dissolved laminarin was undetectable by epitope immunostaining, even after concentrating 100 L seawater (Vidal-Melgosa et al. unpublished). We hypothesize that the turnover of laminarin is very high and corresponds to a major fraction of the overall fixed and respired organic carbon in the surface ocean.

To elucidate major pathways of marine organic carbon, we aim to construct a model of laminarin across multiple trophic levels. To collect the data for our model, we sampled hourly at three stations in the Upwelling System off NW Africa for 25 hours each. We collected size fractions of 0.2 µm to 200 µm mesh size, specifically sampled POC and dissolved organic carbon (DOC), fixed additional 0.2 µm filters for fluorescence *in situ* hybridization (FISH), and tested a new glycan extraction technique. Moreover, once every 6 hours, POC, DOC, 3 µm and 0.2 µm size fractions, and glycan extracts were collected from five CTD-depths; surface, chlorophyll maximum, 100 m, 200 m, and 500 m (Table 3.3). The collected biological data, enriched with oceanographic parameters, will serve to construct a model of dissolved and particulate laminarin concentrations and ecological drivers as the phytoplankton, zooplankton, and bacterial community. From the model, we will deduce the production, release, and degradation of laminarin. The results will provide quantitative estimates

of laminarin fluxes and significantly advance our biogeochemical understanding of organic carbon turnover in the water column.

Table 3.3: CTD deployments for depth profiles during 25 hour sampling. Up to five depths were sampled with the CTD rosette, always including chlorophyll maximum and surface. CTD water was filtered for FISH (3 µm mesh size, 47 mm filter diameter, 1.5 L; 0.2 µm, 47 mm, 1 L; 0.2 µm, 25 mm, 50 ml formalin fixed), POC (>0.47 µm, 47 mm, 1.5 L), DOC (<0.47 µm, 20 ml acidified sample in vial), and glycan extraction (diols, 200 ml pre-filtered at 0.47 µm, 10 ml extract in tube).

Station GeoB-	Date 2019	Start [UTC]	Latitude (N)	Longitude (W)	Depth [m]	Profile Depth [m]
23601_07	21.01	10:00	21°12.53	20°52.23	4170	500
23601_18	21.01	16:01	21°11.51	20°52.28	4152	500
23601_26	21.01	22:00	21°09.79	20°53.82	4155	500
23601_35	22.01	04:02	21°09.25	20°53.74	4160	500
23603_03	25.01	10:00	20°48.30	17°44.31	709	500
23603_12	25.01	16:02	20°48.63	17°44.78	778	500
23603_21	25.01	21:59	20°47.89	17°43.65	636	500
23603_28	26.01	04:00	20°49.16	17°44.52	749	500
23610_12	27.01	10:01	20°46.72	17°25.65	59	50
23610_21	27.01	16:02	20°46.76	17°25.55	59	50
23610_26	27.01	21:59	20°46.56	17°25.48	58	50
23610_29	28.01	03:52	20°46.71	17°25.37	58	50

Sampling

We conducted our sampling along a gradient from the shelf to the open ocean in the Canary Current Upwelling System. Station GeoB-23610 corresponded to the shelf, GeoB-23603 to the slope, and GeoB-23601 to the open ocean station (Table 3.3 and Table 3.4). Series of hourly collected samples were started at 9 am on January 25, January 27, and January 20, respectively, and finished at 9 am on the following day. CTD-rosettes were cast at each station at 10 am, 4 pm, 10 pm, and 4 am.

Zooplankton samples were collected using a handnet with a 0.162 m^2 opening and a 200 µm mesh size (Fig. 3.2). For sampling, a weight was attached to the handnet to permit vertical submersion into the water column. The handnet was lowered to 10 m depth and recovered immediately, sampling the > 200 µm fraction of 1,620 L surface water. The sample was concentrated in a cylinder attached to the bottom of the handnet with 150 µm mesh size by flushing with seawater from the outside of the handnet. Material collected in the cylinder was flushed into a clean wide-neck Kautex bottle and fixed with 2% formaldehyde. Zooplankton in these samples will be analyzed with a focus on the identification and quantification of diatom grazers.

Fig. 3.2: Zooplankton hand net with weight attached.

Phytoplankton samples were collected by filtering 10 L of seawater from the ship inlet at approx. 5 m depth through a 10 µm mesh. Material was flushed with 20 ml 0.47 µm filtered seawater from the mesh into 50 ml Sarstedt tubes and fixed with 1% formaldehyde. Phytoplankton samples will be analyzed microscopically with a focus on identification and quantification of diatoms.

Particle attached prokaryotes were sampled by filtering 1.5 L of seawater from the ship inlet or CTD-bottles onto a 3 µm polycarbonate filter. The flow through was used to sample free-living prokaryotes by filtering through a 0.2 µm polycarbonate filter. Filters were frozen immediately in sterile 2 ml microtubes at -80°C.

Additional 50 ml of seawater from the ship inlet and CTD-bottles were fixed in 1% formaldehyde for 6 hours at 4°C after each CTD cast and filtered onto 0.2 µm polycarbonate filters with cellulose-nitrate filters as stent. The filters were rinsed with 10 ml filtered seawater to remove residual formaldehyde to avoid over-fixation. Filters were stored in small petri dishes covered with parafilm at -20°C. These filters will be analyzed by CARD-FISH to enumerate the microbial community.

Fig 3.3: POC filter with plenty of particulate material. 50 L of seawater from the ship inlet were filtered using a peristaltic pump through 0.47 µm GF/F filters with a diameter of 142 mm.

Hourly POC samples were collected by filtering 50 L through pre-combusted 0.47 µm GF/F filters with 142 mm diameter (Fig 3.3). After filtration, the filters were frozen immediately at -80°C. POC from CTD-depths was sampled by filtering 1.5 L through pre-combusted 0.47 µm GF/F filters with 47 mm diameter. For DOC, 20 ml of flow through were collected in pre-combusted glass vials and 26 µl of 25% HCl added. DOC samples were stored at room temperature for the duration of the cruise and transferred to a solvent free fridge at 4°C. POC will be quantified using an elemental analyzer. Laminarin in the POC fraction will be extracted by heat extraction at 60°C for 60 mins and quantified using enzymatic digestion and subsequent reducing sugar assay (Becker et al. 2017). DOC will be quantified on a Shimadzu TOC analyzer by total combustion.

Glycan extraction was performed using phenyl boronate columns on 200 ml seawater pre-filtered at 0.47 µm through pre-combusted GF/F filters hourly from the ship inlet and from CTD-bottles (Fig. 3.4). In brief, water samples were alkalified to pH 9.5, glycans bound to phenyl boronate gel at high pH, and non-bound residuals washed off with 20 ml MilliQ-water. Glycans were eluted from phenyl boronate gel by decreasing the pH to approx. 4.5. Extracts of 10 ml were collected in 15 ml Sarstedt tubes and frozen at -20°C.

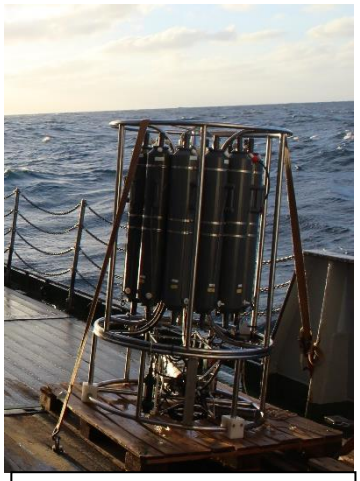

Fig. 3.4: CTD rosette ready for deployment.

Table 3.4: List of sampled stations comprising physical parameters and schedule of sample collection. All 25 hours sampling period started at 9 am. Physical values present mean over sampling period and standard deviation. Temperature, salinity, and fluorescence are surface measurements. Descriptions of collected samples include mesh size cutoff and volumes of seawater processed. All samples except zooplankton were taken from ship inlet.

Station	Date	21.-22. Jan 2019	25.-26. Jan 2019	27.-28. Jan 2019

	Station (Ship)	POS531_1	POS531_3	POS531_10
	Station (Geomar)	GeoB23601	GeoB23603	GeoB23610
Physical parameters	**Region**	**Open**	**Slope**	**Shelf**
	Depth [m]	4150±33	712±39	58.5±0.5
	Temperature [°C]	20.92±0.05	17.96±0.18	17.00±0.16
	Salinity [PSU]	36.75±0.01	36.14±0.03	35.95±0.01
	Fluorescence [g L^{-1} Chl-a]	52.68±1.49	57.84±2.85	58.50±1.50
Samples collected	**Sampling period**	**25 hours**	**25 hours**	**25 hours**
	POC (>0.47 µm, 50 L)	hourly	hourly	hourly
	DOC (<0.47 µm, 20 mL)	hourly	hourly	hourly
	Zooplankton (>150 µm, 1,600 L)	hourly	hourly	6 times overall
	Phytoplankton (>10 µm, 10 L)	hourly	hourly	hourly
	Particles (>3 µm, 1.5 L)	hourly	hourly	hourly
	Free-living microbes (>0.2 µm, 1 L)	hourly	hourly	hourly
	Glycans (diols, 200 mL)	hourly	hourly	hourly

Incubations with ^{13}C-bicarbonate were performed over each 25 h sampling period. 500 ml seawater from the ship inlet were spiked to a final concentration of approx. 10% using ^{13}C-sodium bicarbonate and incubated for 12 h on deck under an “ocean blue” foil with constant seawater flow around incubation bottles from the ship inlet. After sundown, half of the incubations were stopped, 6 ml of water was killed with 100 µl $HgCl_2$ in a head space-free exetainer, and the remaining sample filtered onto a pre-combusted 0.47 GF/F filter. Filters were frozen at -20°C. The remaining half of the incubations were processed in the same way before sunrise after 24 h. $HgCl_2$ killed samples will be used to determine the labeling percentage of the DIC pool, while the filters will be used to determine the uptake of ^{13}C-DIC into biomass, which will allow determination of primary production rates.

3.3 Particle Flux Studies - Upper ocean particle flux measured with free-drifting sediment traps

(Steffen Swoboda, Arjun Chennu, and Morten Iversen)

Background

Lateral transport processes from ocean margins to offshore regions can cause substantial decoupling of surface water productivity and material reaching the open ocean seafloor (Karakas et al., 2009, Iversen et al., 2010). However, conventional deep ocean sediment traps and benthic lander measurements average all settling particles and do not differentiate between particles transported vertically and horizontally. It is therefore difficult to predict the relative contribution of 'fresh' organic material arriving from vertical fluxes of fast-settling particle versus the 'older' organic matter within slowly-sinking particles transported laterally over long distances. Lateral transport from the shelfs to the open ocean are especially pronounced in Eastern Boundary Upwelling Ecosystems (EBUEs) where upwelling is driven by alongshore winds, leading to offshore advection of surface water, which is replaced by colder and nutrient-rich subsurface waters. The EBUEs are characterized by the occurrence of large filaments with high chlorophyll concentrations that can be transported as far as 450 km offshore (Fischer et al., 2009). The aim of this study was to focus on the vertical flux characteristics of particles collected from the slope and offshore region. By analysing particle flux at different depths and linking this data with the other particle experiments, we investigated the impact of lateral transport and upwelling on the settling of marine snow particles.

Sampling

We used an array of free-drifting sediment traps to measure the export fluxes at 100 m, 200 m, and 400 m depth (Table 3.5, Fig. 3.5).

Table 3.5 Deployments of drifting sediment trap.

Action [#]	GeoB [#]	Date [MM-DD]	Time [UTC]	LAT [°N]	LONG [°W]	Water depth [m]
Depl. DF-20	26301_06	21-01	09:06	21° 12,561'	020° 52,499'	4153.4
Rec. DF-20	26301_41	22-01	09:12	21° 07,084'	020° 53,266'	4155.9
Depl- DF-21	26303_01	25-01	09:03	20° 48,426'	017° 44,550'	739.7
Rec- DF-21	26303_35	26-01	08:49	20° 49,989'	017° 43,903'	706.4
Depl. DF-22	26313_01	29-01	08:07	20° 50,948'	018° 44,224'	2693.1
Rec- DF-22	26313_12	30-01	08:42	20° 51,022'	018° 54,835'	3095.1

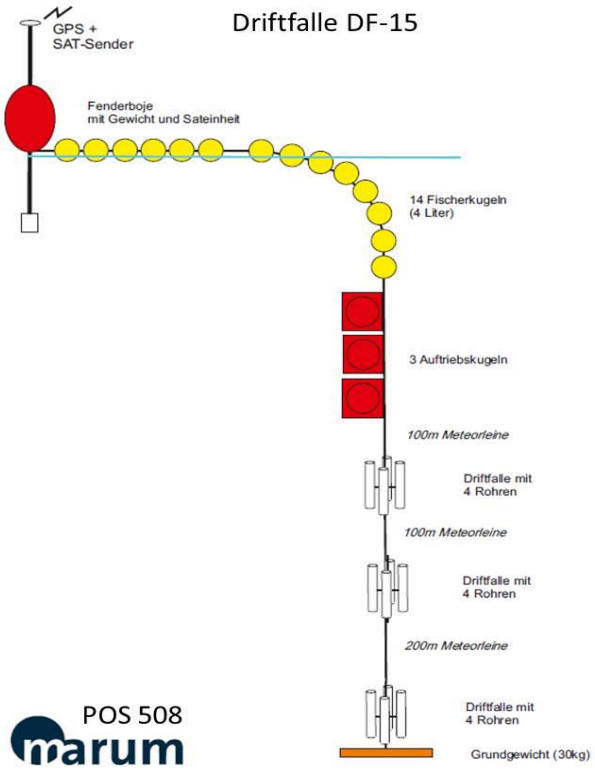

Fig. 3.5 Schematic of the deployments of the drifting arrays DF-20, DF-21, and DF-22. Each array consisted of three trap array with four traps at each. The trap arrays were placed at 100, 200 and 400 m water depth (see also Table 3.5).

Each collection depth had a trap station that consisted of four cylindrical collection tubes with a gyroscopical attachment (Fig. 3.6). Three of the four collection cylinders at each depth were used to collect samples for biogeochemical measurements of total dry weight, particulate organic carbon, particulate organic nitrogen, particulate inorganic carbon, and silica. The fourth trap cylinder at each depth was equipped with a viscous gel that preserved the structure, shape and size of the fragile settling particles.

Fig 3.6: The four gyroscopically mounted sediment trap collection tubes.

After recovery of the drifting trap, two of the samples collected for biogeochemical measurements were fixed with mercury chloride while the third samples collection for biogeochemical measurements was frozen for later analysis in the home laboratory. The particles collected in the gel traps were photographed with a digital camera and a hyperspectral line camera on board and frozen for further detailed investigations in the home laboratory (Fig. 3.7). The image analyses of the gel traps will be used to determine the composition, abundance and size distribution of the sinking particles.

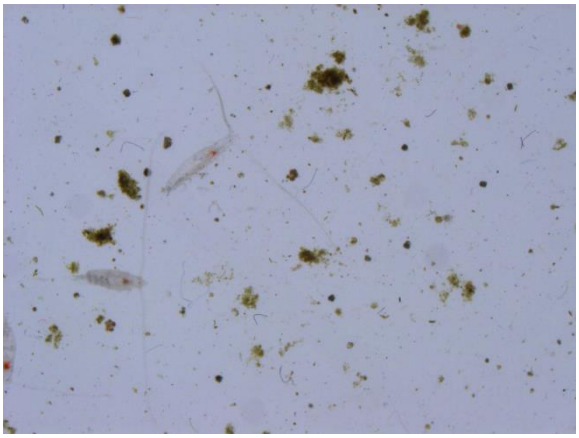

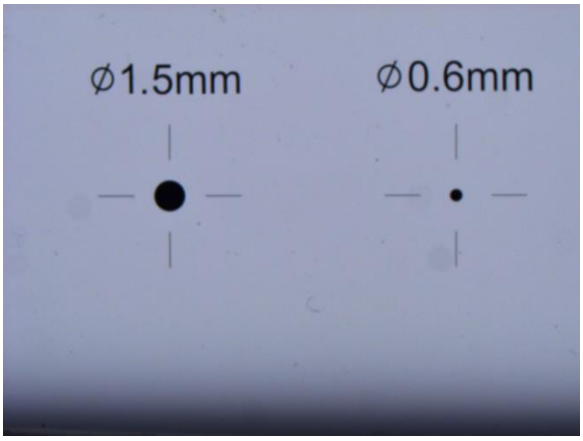

Fig. 3.7: Upper panel shows an image of the collected particles in the gel-trap. The lower panel provide the scale, the large black circle has a diameter of 1.5 mm and the smaller black circle has a diameter of 0.6 mm.

The samples collected for biogeochemical measurements will be used to determine mass fluxes of carbon, nitrogen, biogenic opal, calcium carbonate, and lithogenic material. The different particle types collected in the gel cylinder were photographed using a digital camera and will be used to create particle size distribution of the flux and to identify transformation processes between the different trap depths. Three deployments were carried out during the cruise (DF-20, DF-21, and DF-22, Table 3.5).

The composition of marine snow aggregates is highly dependent on species composition, inorganic components and the state of degradation due to age. Conventional methods to assess the composition of aggregates are often time consuming and invasive which thus limits the use of a single aggregates to one singular analysis. With the help of hyperspectral imaging, it is possible to picture a broader spectrum of reflected light which holds potential to visualize processes that are not visible with conventional cameras or human vision. We therefore investigated the spectra of in-situ collected aggregates and sediments with this non-invasive approach to identify features which could be linked to properties of a sample's composition. The hyperspectral setup consisted of a custom-built H frame with a motor sled placed on the horizontal bar, on which the hyperspectral line camera and lights for improved illumination where attached to.

In-situ aggregates which were embedded in the gel cups from the drifting trap (DF-20, DF-21, and DF-22) where used to take hyperspectral images. Further, sandy sediments from the upper 1 cm of the two sediment stations (see 3.6) were collected using a cut off syringe and placed in petri dishes for hyperspectral imaging. Imaged samples where then stored and will be analysed using established methods in order to link potential features in the spectra to properties of the aggregates and sediments composition.

3.4 Optical Particle Studies - Vertical profiles of marine snow aggregates with the In Situ Camera (ISC)

(Steffen Swoboda and Morten Iversen)

System description

The In Situ Camera (ISC) consisted of an industrial camera with removed infrared filter (from Basler). The camera was connected to a single board PC (Raspberry Pi) and a fixed focal length lens (16mm Edmund Optics), as well as a DSLR camera with a 50mm prime lens and a remotely operated flash. Further, a seabird CTD was attached. Custom made electronics in the system provided power configuration and timing. Furthermore a DSPL battery (24V, 38Ah) was used to power the CTD and Infrared camera system (Fig. 3.8). The Raspberry Pi was both used as the operating system for the infrared camera and to acquire the images from the camera and send them to a SSD hard drive where they were stored. The illumination was provided by a custom made light source that consisted of infrared LEDs which were placed in an array in front of the camera. With this geometrical arrangement of the camera and the light source we obtained shadow images of particles through the water column. The field of view was 24x36 mm and a depth of field of ~24 mm resulting in a volume of approx. 20 ml. We captured 2 images per second and lowered the ISC with 0.3 meters per second (lowest possible speed of winch), which resulted in a total imaged water volume of 120 ml per meter for the infrared camera.

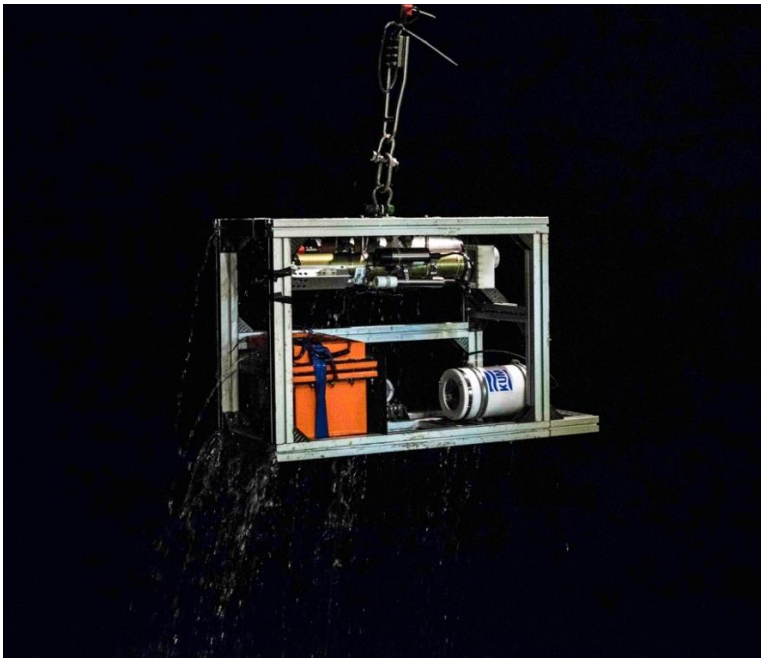

Fig 3.8 Deployment of the In-Situ camera (ISC), consisting of an industrial infrared camera and lens with electronics, an infrared light source and the DSPL battery as well as a DSLR camera with a separate flash.

The DSLR camera and flash were each mounted in respective custom-built pressure housings, and were connected by a cable. The flash was positioned perpendicular to the DSLR camera, so it illuminated the area within the depth of field

from a 90° angle. The camera was set to take 1 image every 3 seconds, resulting in approx. 1 image per lowered meter.

We lowered the ISC to 10 m and waited one minute before we started the profile. This was to avoid air-bubbles in the images captured in the upper 20 m. We further left the camera some minutes at the maximum water profile depth to image particles in a larger water volume, which will allow us to estimate the statistical errors induced by the relatively small water volume captured per depth.

Sampling

We made 33 vertical profiles with the In Situ Camera (ISC). The vertical profiles were down to 500 m where possible (Table 3.6).

Table 0.6: List of In Situ Camera profiles including station number, latitude, longitude, full water depth, and the deployment depth of the in Situ Camera.

Station No. GeoB	Latitude [N]	Longitude [W]	Water depth [m]	Deployment depth [m]
23601_02	21°12.60	20°52.52	4151.3	500
23601_03	21°12.58	20°52.51	4162.7	500
23601_15	21°12.09	20°52.16	4187.1	500
23601_20	21°10.84	20°52.81	4152.4	500
23601_24	21°09.99	20°53.56	4152.8	500
23601_37	21°08.88	20°53.57	4149.1	500
23601_43	21°06.87	20°53.18	4140.8	500
23602_06	20°46.31	17°10.91	27.3	25
23602_18	20°46.34	17°10.88	28.7	25
23603_09	20°48.26	17°44.60	748.9	500
23603_15	20°48.71	17°44.44	727.3	500
23603_19	20°48.02	17°43.86	654.8	500
23603_31	20°49.33	17°44.40	759	500
23603_37	20°49.78	17°43.60	688.7	500
23604_01	20°48.55	17°40.60	430.1	425
23605_02	20°47.97	17°37.79	94.3	90

23606_01	20°47.38	17°31.72	76	70
23607_02	20°46.32	17°19.36	45.7	40
23608_01	20°46.25	17°14.41	39	35
23609_02	20°46.37	17°11.00	28.3	25
23610_15	20°46.64	17°25.54	58.5	50
23610_23	20°46.71	17°25.46	59.5	55
23610_25	20°46.54	17°25.48	58	50
23610_31	20°46.74	17°25.37	58.5	50
23611_02	20°50.08	18°04.51	1573.2	500
23612_01	20°50.86	18°24.20	2100	500
23613_03	20°50.98	18°44.56	2714.5	500
23613_06	20°50.87	18°44.87	2724.2	500
23613_08	20°50.30	18°47.55	2799.2	500
23613_09	20°51.22	18°48.78	2859.2	500
23613_11	20°50.83	18°53.75	3061.8	500

3.5 Marine Microbiology - Size-specific sinking velocity and microbial respiration

(Steffen Swoboda and Morten Iversen)

Background

The majority of marine particulate matter is present in the form of conglomerated particles, composed of phytoplankton, detritus, inorganics and fecal pellets. These are commonly referred to as marine snow (aggregates with equivalent spherical diameters larger than 0.5mm) and are an important part of the marine carbon cycle as they transport photosynthetically fixed carbon from the ocean's surface to the deep. However, the amount of carbon transported to depth is dependent on the relationship between the settling speed and biological degradation of an aggregate. Being composed of various organics, marine snow particles harbour a rich community of living organisms such as bacteria, phytoplankton and small heterotrophs. These organisms degrade the marine snow and are able to recycle the majority of an aggregate before it reaches deeper layers. Inorganic components such as dust or sand grains, however, can be incorporated and add ballast to the marine snow. This result in higher settling velocities and thereby to a more efficient transport to depth. By

knowing the settling speed, particle composition and biological degradation of the marine snow, it is possible to estimate recycling and export of marine snow carbon. The aim of the experiments carried out on board was to assess the composition of particles and the relationship between settling and microbial degradation of settling aggregates in the coastal, at the shelf and in the open ocean. By combining these experiments and results with vertical size-distribution and abundance of aggregates (see section 3.4), we can provide an estimate of carbon attenuation and export from in the three different ocean regions.

Methods and sampling

A Marine Snow Catcher (MSC, from OSIL) was deployed at each station below the Chl. *a* maximum to collect in situ formed marine snow (Table 3.7). The MSC consists of a cylinder with 100 l capacity as upper part and a removable bottom section where caught aggregates can settle into. After deployment, sampled aggregates where left to settle into the bottom section for at least 2 h before gently draining the upper part. Afterwards, the lower section was detached, and aggregates could be hand-picked. A flow chamber with a mounted microscope and oxygen micro profiler was used to measure size, settling and respiration of ~ 20 aggregates per sample site (Fig. 3.9).

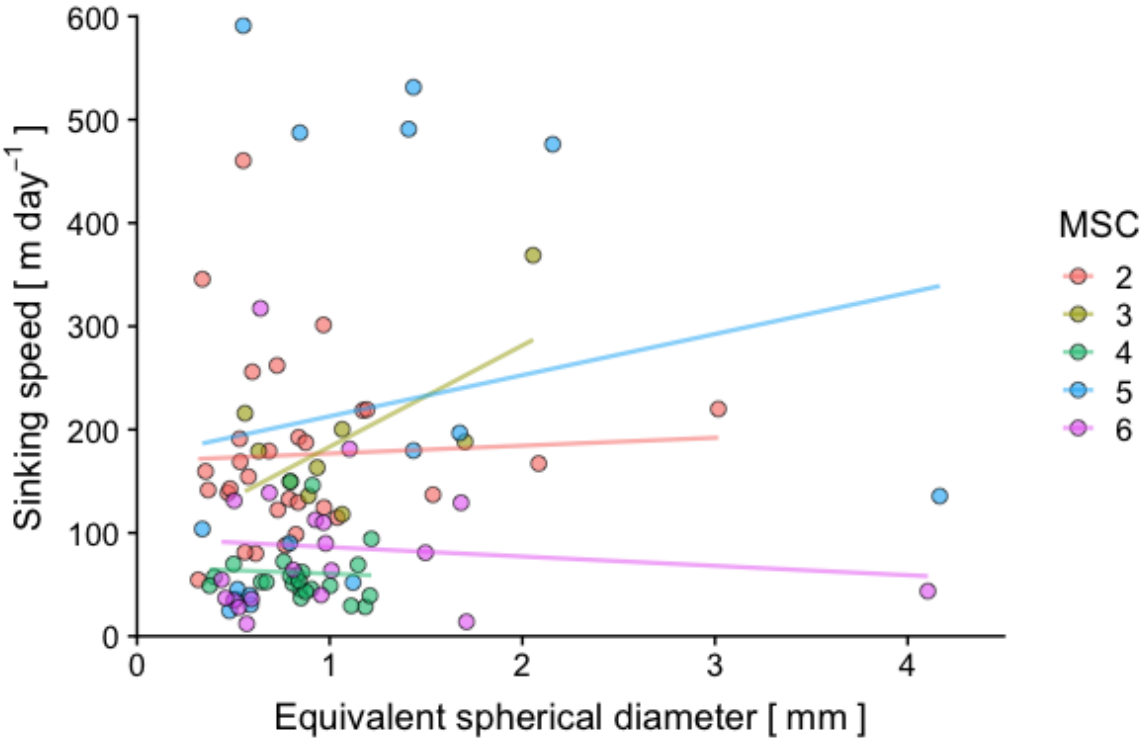

Fig. 3.9 Aggregate sinking velocity as a function of aggregate size from respective sampling sites. Aggregates were collected with the marine snow catcher (MSC) and analysed on board with the flow chamber setup.

Particle composition of individual aggregates was investigated and imaged microscopically. We measured oxygen consumption in the dark and light using oxygen microsensors. Afterwards, individual aggregates where frozen in seawater and stored for analyses of their chemical composition.

Table 3.7 Deployments of the Marine Snow Catcher (MSC) and assessed parameters

Number	GeoB	Date 2019	Time	LAT	LONG	Water depth
[#]	[#]	[MM-DD]	[UTC]	[°N]	[°W]	[m]
1	26301_12	21-01	12:52	21° 12,316'	020° 51,919'	4148.2
2	26302_08	23-01	19:19	20° 46,329'	017° 10,912'	27.8
3	26302_19	24-01	11:08	20° 46,345'	017° 10,859'	27.7
4	26303_38	26-01	10:34	20° 49,737'	017° 43,569'	687.9
5	26310_17	27-01	12:41	20° 46,786'	017° 25,525'	58.2
6	26313_05	29-01	12:43	20° 50,973'	018° 44,811'	2711.9

3.6 Benthic Primary Production, Carbon Remineralization and Nitrogen Cycling

(Soeren Ahmerkamp, Hannah Marchant, Kai Schwalfenberg)

Background

Together, the four EBUEs, the Benguela, the Canary, the Californian and the Humboldt Current Systems, cover about 1% of the total ocean area but contribute around 15% to the total marine primary production (e.g. Carr 2002; Behrenfeld and Falkowski 1997). Furthermore, shelf areas make up 8% of the total ocean area and are responsible for 20-30% of the total marine primary production. Despite the fact that 50-70% of the continental shelves are covered by sands, the vast majority of biogeochemical studies have focused on muddy sediments, that cover less than 10% of the total shelf area (Huettel et al. 2014). As a result, little is known about the role of permeable sandy sediments in the global biogeochemical cycles of carbon and nitrogen.

A substantial proportion of the shelf primary production reaches the sandy sediments that cover the shelf beneath them. These sediments are characterized by extremely low total organic carbon contents, and it has been shown that part of the reason for this is that the organic matter remineralization rates in sandy sediments are high. This means that only organic matter transported laterally to the open ocean has the potential to be sequestered. So far, however the role of shelf areas in global carbon burial and nitrogen cycling is poorly constrained. The sediment underlying the study area consists primarily of sandy sediments. Initial studies of nitrogen-loss in this area

were comprised of ex-situ incubations (Sokoll et al. 2016), but so far no in-situ studies have been carried out in in the region, nor were remineralization determined.

During this cruise we aimed to carry out in situ studies using the Lance-a lot benthic lander to gain insights into sediment topography, sediment transport, and oxygen penetration depths, parameters which are vital in the interpretation of ex-situ incubations (Ahmerkamp et al. 2015, Marchant et al. 2016, Ahmerkamp et al. 2017). Furthermore, we aimed to determine the role that benthic primary producers might play a role in supplying organic matter to the sediment and determining its physical properties. We aimed to study this by observing the distribution, pigment content, and carbon fixation rates of benthic primary producers in situ and ex situ, using hyperspectral optical systems mounted on Lance-a-Lot and in the laboratory which allows determination of the microscale distribution and dynamics of benthic primary production (Chennu et al. 2013).

Sandy shelf stations and Lander deployments

In order to investigate the biogeochemical processes within sandy sediments, we used an integrated approach combining in situ measurements using a benthic lander (LanceALot, Fig. 3.10) and laboratory experiments to determine nitrogen-loss and carbon remineralization rates. During the POS531 cruise, we focused on two sandy shelf stations at GeoB23602 (28.5 m) and GeoB23610 (60 m). These two stations were picked in order to have contrasting light and current regimes on the seafloor.

On both stations the lander-system LanceALot was successfully deployed for 24 hours. The lander was developed to investigate benthic biogeochemical process in highly dynamic shelf systems. LanceALot is equipped with a custom made laser scanner, a hyperspectral camera, a lab-on-a-chip NOx sensor, a 2d-profiling system, acoustic velocimeters (ADV and ADCP) and an eddy correlation system to determine sediment topography, sediment migration, pigment distributions, nitrate concentrations, oxygen penetration depths, current velocities and oxygen fluxes. The measurements are centrally controlled by a NUC-computer which allows for a wireless and autonomous operation.

The two deployment stations were selected based on depth and sediment type. The first, shallow station was located close to the coast in 30 m water depth with mostly coarse sand. The bedforms at this station were relatively large which led to a strong interaction of the topography and the overlying bottom water currents, mainly induced by waves. Therefore, the (preliminary) oxygen fluxes were in the upper range measured for sandy sediments and ranged between ~20-30 mmol m^2 d^{-1}. The second station was located in 60 m water depth and showed only few roughness elements, mostly biogenic mounds. The oxygen fluxes at this station ranged between 10-20 mmol m^2 d^{-1} as a result of a reduced oxygen penetration depths, i.e. weaker ventilation. The images and oxygen data will be further processed in Bremen.

Fig. 3.10: Left panel: LanceALot after a 24 hour deployment on the Mauretanian shelf. Right panel: Surface-scan of the sea-floor using a laser-scanning technique.

Oxygen and N-cycling rates

Sediment was collected at the two lander stations using multiple Van-Veen-Grabs (GeoB23602-09 to GeoB23602-13 and GeoB23610-02 to GeoB23610-11 respectively). On deck, the upper 3 cm of sediment was scraped off the surface of the grab and homogenized. Sediment was then filled into flow through cores (I.D. Ø 10 cm, height 20 cm). Incubations were carried out by exchanging the porewater within the cores from a port at the bottom with water collected from 2 m about the seafloor to which various tracers had been added. After porewater had been exchanged, water was sampled from the port at the bottom of the core over the next 3 – 8 hours using a gas tight glass syringe. Oxygen concentrations were determined immediately using a flow through oxygen optode and water was fixed headspace free in a 6 ml Exetainer (LabCo). 6 time points were taken while oxygen was still present in the porewater and 6 time points were taken at regular intervals after. Oxygen consumption rates were 20 mmol m^{-3} sediment h^{-1} at station GeoB23602, and 110 mmol m^{-3} sediment h^{-1} at station GeoB23610. Exetainers were returned to Bremen for analysis of $^{15}N_2$, $^{15}N_2O$, $^{15}NO_2^-$, $^{15}NO_3^-$ and $^{15}NH_4^+$.

Benthic Primary production rates

2 cm^3 of sediment was sampled from the Van Veen Grab using a cut off syringe and placed into a petri dish. The sediment was subsequently scanned with a hyperspectral image system (as detailed in section 3.3). It was then placed into a 40 ml tube, which was filled with filtered seawater collected from 2 m above the seafloor and incubated with 220 µM ^{13}DIC either in the dark, or in an incubator covered in „Ocean Blue“ foil from Lee filters at in situ temperature on deck. After 24 hours, the sediment was washed to collect any suspended organic material which was subsequently filtered onto a pre-combusted GFF filter and dried. The sediment was collected in an

eppendorf. These samples will be combusted on an EA-GC-IRMS in Bremen to determine the uptake of ^{13}C-DIC into biomass.

Sediment stability

In order to investigate the role that benthic primary producers have in stabilizing sediments, we performed ex situ chamber incubations. For that, a transparent rotating disc was mounted to a MUC core to stir the water above the sediment. At the same time an underwater microscope camera was filming the sediment to determine the onset of sediment movement. Next to the sediment transport, the abundance of benthic primary producers on the sediment surface was measured along a grid with ~1 cm resolution using a photospectrometer. These measurements are complementary to the in situ measurements obtained with LanceALot and will be further analyzed in Bremen to investigate the role of benthic primary producers for sediment stabilization.

FDOM

Incubation experiments were carried out to determine whether production or consumption of FDOM occurred within sediments sampled from GeoB23602 and GeoB23610. Incubations were carried out using MUC cores in a flow through system for sediment cores that were run in parallel to the oxygen and N-cycling flow through cores. The incubation experiments were bases on two MUC cores and two sediment soils. In the MUC cores porewater was sampled through predrilled side ports using rhizones at 0, 2 and 4 cm below the sediment surface. Samples were collected at 0h, 6h, 12h and 24h. In the flow through sediment cores, cores were supplied with unfiltered bottom water at different velocities and samples were taken from the inlet and outlet of the core. Subsequently, porewater flow was halted and further samples were taken after the cores became anoxic. In total 50 samples were collected and will be analysed the FDOM composition.

4 Station list

Station list for the CTD-Rosette (CTD) In Situ Camera (ISC), Zooplankton hand-net (Net), Drifting sediment traps (DF), Secchi Disk (SD), Marine Snow Catcher (MSC), Van der Ween Grab (Grab), The LanceALot lander (LanceALot), the Multicorer for sediment sampling (MUC), and the Bottom Water Sampler (BWS), however, the BWS did not work during the cruise and no samples were obtained.

GeoB-station (#)	Date Time	Device	Latitude (N)	Longitude (W)	Depth (m)
GeoB23601_01	20.01.2019 17:03	CTD	21°12.618	20°52.532	4151.8
GeoB23601_02	20.01.2019 18:52	ISC	21°12.604	20°52.523	4154.1
GeoB23601_03	20.01.2019 18:59	ISC	21°12.597	20°52.526	4153.6
GeoB23601_04	20.01.2019 20:40	Net	21°13.424	20°51.207	4146.8
GeoB23601_05	21.01.2019 09:04	Net	21°12.568	20°52.486	4153.4
GeoB23601_06	21.01.2019 09:06	DF	21°12.561	20°52.499	4153.4
GeoB23601_07	21.01.2019 10:00	CTD	21°12.530	20°52.229	4169.6
GeoB23601_08	21.01.2019 10:04	Net	21°12.539	20°52.207	4161.2
GeoB23601_09	21.01.2019 11:04	Net	21°12.442	20°52.092	4148.6
GeoB23601_10	21.01.2019 11:58	Net	21°12.330	20°51.925	4151.3
GeoB23601_11	21.01.2019 12:08	SD	21°12.340	20°51.891	4170.2
GeoB23601_12	21.01.2019 12:52	MSC	21°12.316	20°51.919	4148.2
GeoB23601_13	21.01.2019 13:05	Net	21°12.315	20°51.910	4149.5
GeoB23601_14	21.01.2019 14:03	Net	21°12.151	20°52.121	4150.1
GeoB23601_15	21.01.2019 14:06	ISC	21°12.152	20°52.123	4149.6
GeoB23601_16	21.01.2019 15:00	Net	21°11.977	20°52.189	4149.8
GeoB23601_17	21.01.2019 15:55	Net	21°11.537	20°52.277	4163.3
GeoB23601_18	21.01.2019 16:01	CTD	21°11.510	20°52.282	4152.1
GeoB23601_19	21.01.2019 17:05	Net	21°11.229	20°52.498	4158.8
GeoB23601_20	21.01.2019 17:32	ISC	21°11.016	20°52.734	4151.1
GeoB23601_21	21.01.2019 18:07	Net	21°10.780	20°52.833	3988.5
GeoB23601_22	21.01.2019 19:02	Net	21°10.494	20°53.010	4153.2
GeoB23601_23	21.01.2019 20:03	Net	21°10.146	20°53.423	4189.5
GeoB23601_24	21.01.2019 20:32	ISC	21°10.092	20°53.489	4153.3
GeoB23601_25	21.01.2019 21:11	Net	21°09.944	20°53.581	4152.3
GeoB23601_26	21.01.2019 22:06	CTD	21°09.787	20°53.826	4152.8
GeoB23601_27	21.01.2019 22:12	Net	21°09.779	20°53.838	4153
GeoB23601_28	21.01.2019 23:07	Net	21°09.786	20°54.132	4163.4
GeoB23601_29	21.01.2019 23:59	Net	21°10.076	20°54.232	4155.6
GeoB23601_30	22.01.2019 00:09	Net	21°10.050	20°54.247	4160
GeoB23601_31	22.01.2019 00:57	Net	21°09.774	20°54.281	4153.9
GeoB23601_32	22.01.2019 01:51	Net	21°09.473	20°54.116	4162.7
GeoB23601_33	22.01.2019 02:47	Net	21°09.475	20°53.951	4151.3
GeoB23601_34	22.01.2019 03:55	Net	21°09.232	20°53.773	4166.4
GeoB23601_35	22.01.2019 04:02	CTD	21°09.250	20°53.738	4159.7
GeoB23601_36	22.01.2019 05:04	Net	21°09.021	20°53.633	4149.9

GeoB23601_37	22.01.2019 06:04	ISC	21°08.906	20°53.556	4148.6
GeoB23601_38	22.01.2019 06:07	Net	21°08.896	20°53.556	4149.3
GeoB23601_39	22.01.2019 07:04	Net	21°08.869	20°53.626	4154.1
GeoB23601_40	22.01.2019 08:02	Net	21°08.758	20°53.511	4150.5
GeoB23601_42	22.01.2019 09:17	Net	21°07.059	20°53.264	4155.2
GeoB23601_43	22.01.2019 09:22	ISC	21°07.034	20°53.282	4224.7
GeoB23602_01	23.01.2019 16:05	Grab	20°46.324	17°11.030	28.6
GeoB23602_02	23.01.2019 16:18	LanceALot	20°46.352	17°11.027	28.7
GeoB23602_03	23.01.2019 17:02	BWS	20°46.317	17°10.924	27.5
GeoB23602_04	23.01.2019 17:23	BWS	20°46.302	17°10.931	27.6
GeoB23602_05	23.01.2019 18:39	BWS	20°46.314	17°10.920	27.5
GeoB23602_06	23.01.2019 18:26	ISC	20°46.314	17°10.917	28.5
GeoB23602_07	23.01.2019 18:55	CTD	20°46.326	17°10.919	28.2
GeoB23602_08	23.01.2019 19:19	MSC	20°46.329	17°10.912	27.8
GeoB23602_09	23.01.2019 19:29	Grab	20°46.334	17°10.904	27
GeoB23602_10	23.01.2019 19:39	Grab	20°46.334	17°10.898	27.8
GeoB23602_11	23.01.2019 19:44	Grab	20°46.339	17°10.903	28.6
GeoB23602_12	23.01.2019 19:50	Grab	20°46.346	17°10.911	27.8
GeoB23602_13	23.01.2019 19:55	Grab	20°46.345	17°10.911	28.8
GeoB23602_14	23.01.2019 20:04	MUC	20°46.345	17°10.914	28.7
GeoB23602_15	23.01.2019 20:13	MUC	20°46.344	17°10.911	27.7
GeoB23602_16	24.01.2019 06:31	Grab	20°46.293	17°10.920	28.1
GeoB23602_17	24.01.2019 09:01	CTD	20°46.324	17°10.912	27.2
GeoB23602_18	24.01.2019 09:41	ISC	20°46.356	17°10.861	26.8
GeoB23602_19	24.01.2019 11:08	MSC	20°46.345	17°10.859	27.7
GeoB23602_20	24.01.2019 12:01	SD	20°46.296	17°10.816	29
GeoB23602_21	24.01.2019 13:30	CTD	20°46.365	17°10.924	29.2
GeoB23603_01	25.01.2019 09:03	DF	20°48.426	17°44.550	739.7
GeoB23603_02	25.01.2019 09:34	Net	20°48.309	17°44.341	712.8
GeoB23603_03	25.01.2019 10:00	CTD	20°48.299	17°44.311	708.8
GeoB23603_04	25.01.2019 10:17	Net	20°48.300	17°44.330	712.2
GeoB23603_05	25.01.2019 11:21	Net	20°48.216	17°44.290	705.7
GeoB23603_06	25.01.2019 12:00	SD	20°48.245	17°44.301	708.2
GeoB23603_07	25.01.2019 12:20	Net	20°48.202	17°44.342	713.7
GeoB23603_08	25.01.2019 13:19	Net	20°48.119	17°44.311	707.2
GeoB23603_09	25.01.2019 14:02	ISC	20°48.208	17°44.607	750.1
GeoB23603_10	25.01.2019 14:19	Net	20°48.250	17°44.603	749.5
GeoB23603_11	25.01.2019 15:21	Net	20°48.520	17°44.810	792
GeoB23603_12	25.01.2019 16:02	CTD	20°48.632	17°44.779	777.9
GeoB23603_13	25.01.2019 16:35	Net	20°48.609	17°44.685	761.7
GeoB23603_14	25.01.2019 17:23	Net	20°48.632	17°44.471	730.1
GeoB23603_15	25.01.2019 17:30	ISC	20°48.661	17°44.454	728.7
GeoB23603_16	25.01.2019 18:21	Net	20°48.681	17°44.422	724.9
GeoB23603_17	25.01.2019 19:22	Net	20°48.542	17°44.339	712.8
GeoB23603_18	25.01.2019 20:20	Net	20°48.233	17°44.091	679.6
GeoB23603_19	25.01.2019 20:31	ISC	20°48.194	17°44.024	671.7
GeoB23603_20	25.01.2019 21:19	Net	20°48.003	17°43.763	646.1
GeoB23603_21	25.01.2019 21:59	CTD	20°47.893	17°43.648	636

GeoB23603_22	25.01.2019 22:21	Net	20°47.826	17°43.620	632.6
GeoB23603_23	25.01.2019 23:23	Net	20°47.981	17°43.745	645.2
GeoB23603_24	26.01.2019 00:18	Net	20°48.111	17°43.945	664.2
GeoB23603_25	26.01.2019 01:21	Net	20°48.296	17°44.027	676
GeoB23603_26	26.01.2019 02:20	Net	20°48.290	17°44.190	694.7
GeoB23603_27	26.01.2019 03:19	Net	20°48.511	17°44.307	712.6
GeoB23603_28	26.01.2019 04:00	CTD	20°49.157	17°44.520	748.8
GeoB23603_29	26.01.2019 04:23	Net	20°49.172	17°44.484	747.1
GeoB23603_30	26.01.2019 05:18	Net	20°49.216	17°44.505	750
GeoB23603_31	26.01.2019 06:01	ISC	20°49.292	17°44.378	753
GeoB23603_32	26.01.2019 06:20	Net	20°49.315	17°44.393	759.8
GeoB23603_33	26.01.2019 07:19	Net	20°49.440	17°44.314	741
GeoB23603_34	26.01.2019 08:13	Net	20°49.816	17°44.170	725.8
GeoB23603_36	26.01.2019 09:21	Net	20°49.898	17°43.689	692.4
GeoB23603_37	26.01.2019 09:31	ISC	20°49.879	17°43.653	690.5
GeoB23603_37	26.01.2019 09:36	ISC	20°49.868	17°43.640	689.6
GeoB23603_38	26.01.2019 10:34	MSC	20°49.737	17°43.569	687.9
GeoB23604_01	26.01.2019 11:31	ISC	20°48.522	17°40.589	428.8
GeoB23604_02	26.01.2019 12:15	CTD	20°48.591	17°40.575	421.7
GeoB23605_01	26.01.2019 13:36	CTD	20°47.829	17°37.692	93.8
GeoB23605_02	26.01.2019 13:59	ISC	20°47.955	17°37.767	94
GeoB23606_01	26.01.2019 15:36	ISC	20°47.358	17°31.721	76.2
GeoB23606_02	26.01.2019 15:54	CTD	20°47.387	17°31.729	75.9
GeoB23607_01	26.01.2019 17:30	CTD	20°46.315	17°19.348	46.5
GeoB23607_02	26.01.2019 17:50	ISC	20°46.304	17°19.365	46.5
GeoB23608_01	26.01.2019 18:42	ISC	20°46.251	17°14.404	39.1
GeoB23608_02	26.01.2019 18:55	CTD	20°46.256	17°14.409	38.1
GeoB23609_01	26.01.2019 19:56	CTD	20°46.342	17°11.025	28.3
GeoB23609_02	26.01.2019 20:15	ISC	20°46.372	17°11.007	28.1
GeoB23609_03	26.01.2019 20:24	Grab	20°46.384	17°10.989	28.3
GeoB23610_01	27.01.2019 07:58	CTD	20°46.620	17°25.680	59.2
GeoB23610_02	27.01.2019 08:32	Grab	20°46.638	17°25.704	59.2
GeoB23610_03	27.01.2019 08:41	Grab	20°46.625	17°25.703	59.2
GeoB23610_04	27.01.2019 08:48	Grab	20°46.635	17°25.693	59.7
GeoB23610_05	27.01.2019 08:55	Grab	20°46.630	17°25.696	59.2
GeoB23610_06	27.01.2019 09:02	Grab	20°46.633	17°25.683	59.2
GeoB23610_07	27.01.2019 09:09	Grab	20°46.625	17°25.693	59.2
GeoB23610_08	27.01.2019 09:16	Grab	20°46.621	17°25.720	59
GeoB23610_09	27.01.2019 09:21	Grab	20°46.636	17°25.721	59.5
GeoB23610_10	27.01.2019 09:27	Grab	20°46.621	17°25.713	59.5
GeoB23610_11	27.01.2019 09:33	Grab	20°46.622	17°25.699	60
GeoB23610_12	27.01.2019 09:58	CTD	20°46.715	17°25.645	58.7
GeoB23610_13	27.01.2019 10:15	Net	20°46.718	17°25.666	59
GeoB23610_14	27.01.2019 10:26	LanceALot	20°46.654	17°25.675	59.2
GeoB23610_15	27.01.2019 10:51	ISC	20°46.635	17°25.555	58.5
GeoB23610_16	27.01.2019 12:01	SD	20°46.706	17°25.498	59
GeoB23610_17	27.01.2019 12:41	MSC	20°46.786	17°25.525	58.2
GeoB23610_18	27.01.2019 13:02	ISC	20°46.762	17°25.506	59

GeoB23610_19	27.01.2019 14:34	MUC	20°46.835	17°25.515	58.5
GeoB23610_20	27.01.2019 14:43	MUC	20°46.850	17°25.507	59.5
GeoB23610_21	27.01.2019 16:02	CTD	20°46.755	17°25.547	59.2
GeoB23610_22	27.01.2019 16:20	Net	20°46.754	17°25.517	58.7
GeoB23610_23	27.01.2019 16:41	ISC	20°46.718	17°25.462	58.7
GeoB23610_24	27.01.2019 20:41	Net	20°46.548	17°25.442	58.2
GeoB23610_25	27.01.2019 21:00	ISC	20°46.523	17°25.474	58.5
GeoB23610_26	27.01.2019 21:59	CTD	20°46.559	17°25.484	57.5
GeoB23610_27	27.01.2019 22:16	Net	20°46.568	17°25.498	59.2
GeoB23610_28	27.01.2019 23:06	Net	20°46.536	17°25.480	58
GeoB23610_29	28.01.2019 03:52	CTD	20°46.711	17°25.367	58
GeoB23610_30	28.01.2019 04:17	Net	20°46.733	17°25.351	58.2
GeoB23610_31	28.01.2019 04:19	ISC	20°46.738	17°25.353	58.2
GeoB23610_32	28.01.2019 04:33	Grab	20°46.719	17°25.369	58
GeoB23611_01	28.01.2019 15:21	CTD	20°50.047	18°04.525	1318.9
GeoB23611_02	28.01.2019 16:49	ISC	20°50.053	18°04.530	1570.5
GeoB23612_01	28.01.2019 20:28	ISC	20°50.808	18°24.201	2098.2
GeoB23612_02	28.01.2019 21:17	CTD	20°50.827	18°24.222	2098.9
GeoB23613_01	29.01.2019 08:07	DF	20°50.948	18°44.224	2693.1
GeoB23613_02	29.01.2019 08:43	CTD	20°50.976	18°44.219	2692
GeoB23613_03	29.01.2019 10:04	ISC	20°51.084	18°44.493	2712.4
GeoB23613_04	29.01.2019 11:59	SD	20°51.027	18°44.737	2713.2
GeoB23613_05	29.01.2019 12:43	MSC	20°50.973	18°44.811	2711.9
GeoB23613_06	29.01.2019 13:09	ISC	20°50.944	18°44.816	2724
GeoB23613_07	29.01.2019 14:04	CTD	20°50.751	18°45.045	2715
GeoB23613_08	29.01.2019 16:29	ISC	20°50.303	18°47.460	2802
GeoB23613_09	29.01.2019 20:30	ISC	20°51.155	18°48.735	2862.5
GeoB23613_10	29.01.2019 21:24	CTD	20°51.260	18°48.830	2847.8
GeoB23613_11	30.01.2019 07:02	ISC	20°50.795	18°53.648	3121.2

5 Ackownledgements

This cruise was funded by the DFG Research Center and the Excellence Cluster at MARUM, University of Bremen. The R/V POSEIDON was again a perfect platform to perform our yearly time-series and process studies, including some testing of newly developed optical instruments. We thank Captain M. Günther and his entire crew for their professional and excellent support during the cruise. We are also indebted to the German Authorities for Foreign Affairs in Berlin, the authorities in Rabat (Morocco) and the authorities in Nouakchott (MRT) that supported us to get research permissions during the planning phase of the cruise.

6 References

Ahmerkamp S., Winter C., Janssen F., Kuypers M. M., & Holtappels M. (2015). The impact of bedform migration on benthic oxygen fluxes. Journal of Geophysical Research: Biogeosciences, 120(11), 2229-2242.

Ahmerkamp S., Winter C, Krämer K., de Beer D., Janssen F., Friedrich J., Kuypers M. M., Holtappels M. (2017). "Regulation of benthic oxygen fluxes in permeable sediments of the coastal ocean." Limnology and oceanography 62(5): 1935-1954.

Becker S., Scheffel A., Polz M. F., Hehemann J.-H. (2017) Accurate Quantification of Laminarin in Marine Organic Matter with Enzymes from Marine Microbes. *Appl Environ Microbiol*, 83.

Behrenfeld M. J., Falkowski P. G. (1997) Photosynthetic rates derived from satellite-based chlorophyll concentration. Limnology and oceanography 42(1): 1-20.

Breitbart M. (2012) Marine viruses: truth or dare. *Ann Rev Mar Sci*, 4: 425-48.

Carlson C. A., Hansell D. A. (2015) DOM Sources, Sinks, Reactivity, and Budgets. in, *Biogeochemistry of Marine Dissolved Organic Matter*.

Carr, M.-E., 2002. Estimations of potential productivity in Eastern Boundary Currents using remote sensing. Deep-Sea Res. II 49, 59-80.

Carr M.-E., Kearns E. J. (2003) Production regimes in four Eastern Boundary Current systems. Deep Sea Research Part II: Topical Studies in Oceanography 50(22-26): 3199-3221.

Chennu A., Färber P., Volkenborn N., Alnajjar M., Janssen F., de Beer D., Polerecky L. (2013) Hyperspectral imaging of the microscale distribution and dynamics of microphytobenthos in intertidal sediments. Limnology and Oceanography: Methods 11(10): 511-528.

Fischer G., Reuter C., Karakas G., Nowald N., Wefer G. (2009) Offshore advection of particles within the Cape Blanc filament, Mauritania: Results from observational and modelling studies. Prog. Oceanogr. 83, 322-330.

Huettel M., Wild C., Gonelli S. (2006) Mucus trap in coral reefs: formation and temporal evolution of particle aggregates caused by coral mucus. Mar. Ecol. Prog. Ser. 307, 69-84.

Iversen M.H., Nowald N., Ploug H., Jackson G.A., Fischer G. (2010) High resolution profiles of vertical particulate organic matter export off Cape Blanc, Mauritania: Degradation processes and ballasting effects. Deep-Sea Res. I 57, 771-784.

Karakas G., Nowald N., Schäfer-Neth C., Iversen M.H., Barkmann W., Fischer G., Marchesiello P., Schlitzer R. (2009) Impact of particle aggregation on vertical fluxes of organic matter. Prog. Oceanogr. 83, 331-341.

Marchant H. K., Holtappels M., Lavik G., Ahmerkamp S., Winter C., Kuypers M. M. (2016) Coupled nitrification–denitrification leads to extensive N loss in subtidal permeable sediments. Limnology and oceanography 61(3): 1033-1048.

Sokoll S., Lavik G., Sommer S., Goldhammer T., Muypers M. M., Holtappels M. (2016) Extensive nitrogen loss from permeable sediments off North-West Africa. Journal of Geophysical Research: Biogeosciences 121(4): 1144-1157.

Suttle C. A. (2005) Viruses in the sea, *Nature*, 437: 356-61.

Suttle C. A. (2007) Marine viruses--major players in the global ecosystem, *Nat Rev Microbiol*, 5: 801-12.

Teeling H., Fuchs B. M., Becher D., Klockow C., Gardebrecht A., Bennke C. M., Kassabgy M., Huang S., Mann A. J., Waldmann J., Weber M., Klindworth A., Otto A., Lange J., Bernhardt J., Reinsch C., Hecker M., Peplies J., Bockelmann F. D., Callies U., Gerdts G., Wichels A., Wiltshire K. H., Glockner F. O., Schweder T., Amann R. (2012) Substrate-controlled succession of marine bacterioplankton populations induced by a phytoplankton bloom, *Science*, 336: 608-11.

Unfried F., Becker S., Robb C. S., Hehemann J. H., Markert S., Heiden S. E., Hinzke T., Becher D., Reintjes G., Kruger K., Avci B., Kappelmann L., Hahnke R. L., Fischer T., Harder J., Teeling H., Fuchs B., Barbeyron T., Amann R. I., Schweder T. (2018) Adaptive mechanisms that provide competitive advantages to marine bacteroidetes during microalgal blooms. *ISME J*, 12: 2894-906.